JOURNAL OF SOLID STATE CHEMISTRY 55, 23–29 (1984)

The Luminescence of Mercury-like Ions in and the Crystal Structure of $SrLaBO_4$

HAO ZHIRAN* AND G. BLASSE

Physical Laboratory, State University Utrecht, P.O. Box 80.000, 3508 TA Utrecht, The Netherlands

Received February 22, 1984; in revised form May 1, 1984

The crystal structure of $SrLaBO_4$ contains triangular borate groups. The luminescence of mercury-like ions (Sn^{2+}, Sb^{3+}, Tl^{+}, Pb^{2+}, Bi^{3+}) in this host lattice is characterized by a large Stokes shift. The Pb^{2+} is a very efficient activator at room temperature. The luminescent properties are discussed in terms of earlier models related to an off-center position of the metal ion. The emission of Eu^{3+} shows that the crystal structure has a disordered nature and confirms an off-center position. Energy transfer from Pb^{2+} to Eu^{3+} and Tb^{3+} was studied and found to be inefficient.

1. Introduction

Van de Spijker and Konijnendijk (*1*) have given crystallographic and Pb^{2+} luminescence data for $SrLaBO_4$ and $CaLaBO_4$. They suggest isomorphism with $BaAl_2O_4$, which seems hard to believe in view of the radii of the ions involved. The Pb^{2+} luminescence shows a large Stokes shift and high efficiency at room temperature. In view of earlier work on luminescences of this type in this laboratory (*2*), this seemed to be a tempting case to investigate in more detail. In the course of this study we also investigated the luminescence of other ions in $SrLaBO_4$. The results are interesting from a luminescence as well as a crystallochemical point of view.

2. Experimental

Samples were prepared as described in Ref. (*1*). They were checked by X-ray powder diffraction.

Vibrational spectroscopy and luminescence measurements were performed as described in Ref. (*3*). The infrared and Raman spectra were obtained at room temperature. Infrared spectra were obtained using the KBr-pellet technique. The luminescence spectrometer is a Perkin–Elmer MPF-3A equipped with a helium-flow cryostat. Decay times were measured using a setup described in Ref. (*2*).

3. Results and Discussion

3.1. Vibrational spectra and crystal structure. Table I shows the infrared and Raman spectra together with data for $LaBO_3$ from the literature (*4*). All vibrational frequencies observed below 450 cm^{-1} are ascribed to lattice vibrations, i.e., vibrations of the Sr^{2+} and La^{3+} ions relative to the borate sublattice. Those above 550 cm^{-1} are internal borate vibrations. These results show that the borate group in $SrLaBO_4$ is a

* On leave of absence from Changchun Institute of Physics, Chinese Academy of Sciences, Changchun, P.R. China.

0022-4596/84 $3.00

TABLE I

INFRARED AND RAMAN SPECTRA OF $SrLaBO_4$[a]

$SrLaBO_4$		$LaBO_3$[c]	
Infrared[b]	Raman[b]	BO_3^{3-} (D_{3h})	
~900(br,w)	950,920,905(m)	939	$\nu_1(A_1')$
690(m)	—	741	$\nu_2(A_2'')$
~1200(vs,br)	—	1330	$\nu_3(E')$
590(w)	580(br,m)	606	$\nu_4(E')$
~400(vbr)	440(m)		
	320(s)		
	290(m)		
	240(s)		
	205(w)		
	190(m)		
	175(s)		

[a] All values in cm^{-1}.

[b] Symbols: br = broad, v = very, s = strong, m = medium, w = weak.

[c] From Ref. (*4*).

triangular BO_3^{3-} group like in $LaBO_3$. For tetrahedral BO_4^{5-} groups especially the infrared stretching mode at ~1200 cm^{-1} is expected at considerably lower wavenumbers (1000–1050 cm^{-1}, Ref. (*5*)).

This shows that the original proposal that $SrLaBO_4$ (and $CaLaBO_4$) should have the stuffed tridymite structure ($BaAl_2O_4$) is incorrect, because this implies tetrahedral borate groups. Since $BaAl_2O_4$ has one large and two small ions, and $SrLaBO_4$ two large and one small ion, this proposal was unlikely anyhow.

One of us has shown that $CaYBO_4$ (Ref. (*6*)) is isomorphous with Y_2BeO_4 (Ref. (*7*)). This structure contains BO_3^{3-} (BeO_3^{4-}) groups. The Ca^{2+} and Y^{3+} ions are in octahedral coordination. Note that one of the four oxygen ions has only Y(Ca) neighbors, i.e., no Be(B) neighbors. Although SrLa BO_4 and $CaLaBO_4$ have definitely a different structure, there may exist a stronger analogy than suspected in Ref. (*1*). Again one of the four oxygen ions does not coordinate the boron. The $Sr^{2+}(Ca^{2+})$ and La^{3+} sites have probably a higher coordination than octahedral. Evidence for this follows from the luminescence studies. A structure determination of $SrLaBO_4$ or $CaLaBO_4$ remains necessary to confirm these results and to establish all the other structural details.

3.2. Eu^{3+} luminescence. The luminescence of the Eu^{3+} ion was investigated, because usually the spectra give information on the site symmetry. For $SrLa_{0.97}Eu_{0.03}BO_4$ we observed a bright orange luminescence under ultraviolet excitation at room temperature and below. The spectra contain the well-known transitions within the $4f^6$ configuration of Eu^{3+}. In addition there is a broad and intense excitation band with a maximum at about 300 nm. This corresponds to a charge-transfer transition. Comparison with charge-transfer transitions in different Eu^{3+} complexes shows that (a) octahedral coordination can be excluded, because then the charge-transfer transition should be at about 250 nm, (b) the coordination number is about 10 (Ref. (*8*, *9*)).

Excitation into the charge-transfer transition yields an emission spectrum as given in Fig. 1. We note the following details: (a) the intensity of the $^5D_0$–$^7F_0$ emission line is very high. This shows the presence of a linear crystal field on the Eu^{3+} site (*10*), which indicates an asymmetrical coordination. It may well be that the oxygen ion which does

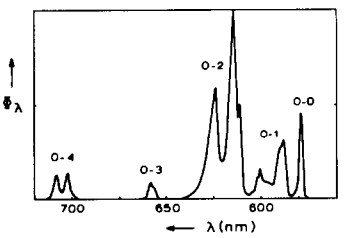

FIG. 1. Spectral energy distribution of the Eu^{3+} emission of $SrLaBO_4$–Eu^{3+} at LHeT, under charge-transfer excitation (~300 nm). The notation $0 \rightarrow J$ denotes the transitions $^5D_0$–^7F_J. The Φ_λ denotes the photon flux per constant-wavelength interval in arbitrary units.

not coordinate boron, plays a role in this effect. (b) The lines are broad. The linewidths observed are not limited by the spectral resolution of the instrument. Especially the $^5D_0$–$^7F_1$ transition is instructive. In first approximation there are two components but each of these contains a whole family of sublines. This leads to the conclusion that the crystal field at the Eu^{3+} site varies from site to site, i.e., the structure is disordered. An obvious possibility for this is disorder between the Sr^{2+} and La^{3+} ions, because these ions have nearly equal ionic radii. It cannot be excluded that these ions occupy even one and the same sublattice. The literature contains many examples of this [e.g., $SrLaAlO_4$ (Ref. (*11*), $SrLaNiNbO_6$ (Ref. (*12*)]. Also in $CaYBO_4$ the Ca^{2+} and Y^{3+} ions are distributed statistically among the two yttrium sublattices (*6*).

That the La^{3+} site is too large for Eu^{3+} becomes also clear from the following. We tried in vain to prepare $SrEuBO_4$ (and $SrGdBO_4$). The X-ray pattern showed a.o. $EuBO_3$. However, even for $SrLa_{0.97}Eu_{0.03}BO_4$ we found indication for a second phase containing Eu^{3+}. The spectra mentioned up until here, are the same for 4.2 and 300 K. If excitation is at about 395 nm, i.e., into $^7F_0 \rightarrow {}^5L_7$, the 300 K emission spectrum is like the one in Fig. 1. The 4.2 K emission spectrum, however, shows a weak, but clear, second $^5D_0 \rightarrow {}^7F_0$ emission line (at lower energy than in Fig. 1) and an additional $^5D_0$–$^7F_1$ emission line in between the two components given in Fig. 1. These extra lines disappear between 50 and 100 K. We assign them to a second Eu^{3+}-containing phase with low quenching temperature of the emission. The $^7F_0 \rightarrow {}^5L_7$ excitation will excite all Eu^{3+} ions in every phase, because they have about equal and low oscillator strength. If the charge-transfer excitation in the second phase is at higher energies than in $SrLaBO_4$, excitation at 300 nm excites mainly the Eu^{3+} ions in $SrLaBO_4$.

This suggests that the structure of $SrLaBO_4$ is only stable for the largest trivalent rare-earth ions.

We were not able to obtain any Eu^{2+} emission from samples $(Sr,Eu)LaBO_4$ prepared in a reducing atmosphere. Only Eu^{3+} luminescence was observed.

3.3. Luminescence of other lanthanides. Two other activators were tried, viz. Ce^{3+} and Tb^{3+}. For a composition $SrLa_{0.97}Ce_{0.03}BO_4$ we observed at 4.2 and 300 K a blue luminescence. The emission exists of a band peaking at 450 nm. It has a weak shoulder at about 420 nm. The excitation spectrum shows a band at 350 nm and some weaker ones at shorter wavelengths. There is a long thermal quenching range, which starts at about 50 K and ends above 300 K.

These spectra are characteristic of Ce^{3+} (Ref. (*13*)). The excitation bands correspond to the crystal-field split $4f \rightarrow 5d$ transitions. The emission is the reverse transition from the lowest crystal-field component to the ground state which is split by about 2000 cm^{-1} ($^2F_{5/2}$–$^2F_{7/2}$). It may well be that the 450- and 420-nm peaks correspond to these two transitions. However, due to the variation in the crystal field as a result of the disordered crystal structure, there may also be different types of Ce^{3+} ions, so that the $^2F_{5/2}$–$^2F_{7/2}$ cannot be observed at all in the spectra.

If the Stokes shift of the emission of $SrLaBO_4$–Ce is compared with those of other phosphors (*14*), it is found that it is fairly large, so that low thermal quenching can be expected. The long quenching region may also indicate the presence of several, slightly different, Ce^{3+} ions.

For $SrLa_{0.97}Tb_{0.03}BO_4$ we observed a green emission. This is hard to excite efficiently with conventional ultraviolet radiation. The spectra contain the well-known transitions within the $4f^8$ shell of Tb^{3+} (Ref. (*13*)). The excitation spectrum shows an $f \rightarrow d$ transition above 250 nm. As for Eu^{3+} the emission lines in the Tb^{3+} spectrum remain

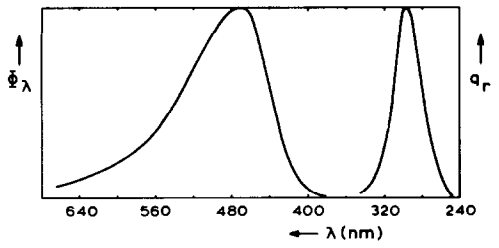

FIG. 2. Emission (left-hand side) and excitation (right-hand side) spectra of the luminescence of $SrLaBO_4$–Sn^{2+} at LHeT. The q_r denotes the relative quantum output.

broad, even for narrow slits. This confirms the interpretation given above.

3.4. Luminescence of mercury-like ions. We observed luminescence for the following ions: $Sn^{2+}(5s^2)$, $Sb^{3+}(5s^2)$, $Tl^{+}(6s^2)$, $Pb^{2+}(6s^2)$, $Bi^{3+}(6s^2)$. Studies were restricted to $SrLaBO_4$, because Pb^{2+} in $SrLaBO_4$ and $CaLaBO_4$ gives essentially the same results. The emission consists of a broad band in the visible. The excitation band is in the short-wavelength ultraviolet, so that the Stokes shift is large. This behavior is illustrated in Figs. 2 and 3 for $SrLaBO_4$–Sn^{2+} and $SrLaBO_4$–Pb^{2+}, respectively.

First we mention some trivial difficulties. It was hard to obtain Tl^{+}- activated samples. Probably the thallium ion with its large size and deviating charge does not fit very well into the lattice. The low Tl^{+} concentration in the samples is the reason for the low light output observed. There is no thermal quenching up until 300 K. The Sb^{3+} ion and

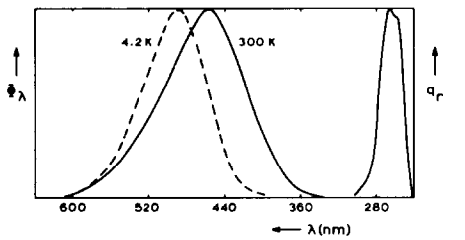

FIG. 3. Emission (left-hand side) and excitation (right-hand side) spectra of the luminescence of $SrLaBO_4$–Pb^{2+} (1%) at 4.2 and 300 K. The excitation spectra for both temperatures coincide.

especially the Bi^{3+} ion prefer the $LaBO_3$ phase which is later washed out (*1*). It was hard to obtain samples with reasonable activator concentrations and without luminescent second phases.

Our results are summarized in Table II. Visually the lead-activated compounds are the most efficient ones, also at room temperature. This is due to the fact that Pb^{2+} can be easily substituted for Sr^{2+} and to the high quantum efficiency (*1*). The spectral characteristics (and efficiency) resemble closely those of the lamp phosphor $Ca_5(PO_4)_3F$–Sb^{3+}. Note from Table II that the Stokes shift increases (and the quenching temperature T_q decreases) in the sequence of $6s^2$ ions Tl^{+}, Pb^{2+}, Bi^{3+}. The same is true for the $5s^2$ ions Sn^{2+}, Sb^{3+}. The Stokes shift is smaller for the $5s^2$ ion than for the corresponding $6s^2$ ion, but T_q is lower.

The large Stokes shifts observed suggest strongly that the mercury-like ions are off-center in $SrLaBO_4$. Unfortunately the structure is not known. Above we presented evidence that the coordination of $La^{3+}(Sr^{2+})$ consists of many anions, part of which are not coordinated to borium. This situation may be favorable for an off-center position.

TABLE II

LUMINESCENT PROPERTIES OF MERCURY-LIKE IONS IN $SrLaBO_4$

Sample[a]	Emission maximum (nm)	Excitation maximum[c] (nm)	T_q (K)
$Sr_{0.98}Sn_{0.02}LaBO_4$	475[b]	295	200
$SrLa_{0.99}Sb_{0.01}BO_4$	465[b]	285	100
$Sr_{0.98}Tl_{0.01}La_{1.01}BO_4$	445	260	>300
$Sr_{0.99}Pb_{0.01}LaBO_4$	460(490)[b]	265	>300
$Sr_{0.95}Pb_{0.05}LaBO_4$	460(490)[b]	275	>300
$Sr_{0.5}Pb_{0.5}LaBO_4$	460(490)[b]	285	>300
$SrLa_{0.99}Bi_{0.01}BO_4$	530[b]	260	250

[a] Starting composition.
[b] At 4.2 K, others 300 K.
[c] All values for 4.2 and 300 K.

In line with this the larger Stokes shift is observed for the smaller, i.e., higher-charged ions. This is most clear from the series Tl^+, Pb^{2+}, Bi^{3+}. The smaller the ion, the more possible an off-center position becomes. Note that the value of the Stokes shift determines also the quenching temperature: the smaller the Stokes shift, the higher T_q (see, e.g., Tl^+, Pb^{2+}, Bi^{3+} in Table II). This follows immediately from the configurational coordinate diagram (*15*).

Relations of this type hold in the series of $6s^2$ ions and in the series of $5s^2$ ions. A comparison between the two series (Table II) shows that the relations are not valid on going from $5s^2$ to $6s^2$. For example, Sb^{3+} is smaller than Bi^{3+}, but has a smaller Stokes shift too. Also T_q is lower. It cannot be excluded that this is due to a difference in bonding. This point is under study in our laboratory. Since the Sn^{2+}- and Pb^{2+}-activated samples were most easily prepared and had the highest light output, we studied these in more detail.

3.5. Pb^{2+} luminescence. The emission spectrum of $SrLaBO_4$–Pb^{2+} shifts to longer wavelengths upon cooling, whereas the excitation spectrum remains essentially the same (see Fig. 3). Exactly the same behavior was observed for $Ca_5(PO_4)_3F$–Sb^{3+} (Ref. (*16*)). Here the shift is from 470 to 515 nm (300 and 4.2 K, respectively). In the halophosphate we are dealing with off-center Sb^{3+} which occurs as an associate $(Sb^{\cdot}_{Ca} \cdot O'_F)^x$. It was suggested that the Sb^{3+} ion goes further off-center, when the temperature is lowered. The same may be true for the Pb^{2+} ion in $SrLaBO_4$.

Further we measured decay times of the Pb^{2+} luminescence. Results are given in Fig. 4. All decay curves were exponential. The data were analyzed with a three-level scheme: level 3 ($^3P_1$) > level 2 ($^3P_0$) > level ($^1S_0$), where the free-atom notation has been used. The drawn line in Fig. 4 is a fit for $\Delta E_{23} = (153 \pm 17)\ cm^{-1}$, $\tau_0 = (540 \pm 13)$ μsec and $\tau_1 = (0.15 \pm 0.1)$ μsec. Here ΔE_{23} is the energy difference between levels 2 and 3 and τ_J the purely radiative decay time of the level ^3P_J. The results are well in line with those observed for Pb^{2+} and Bi^{3+} in off-center position (*2*).

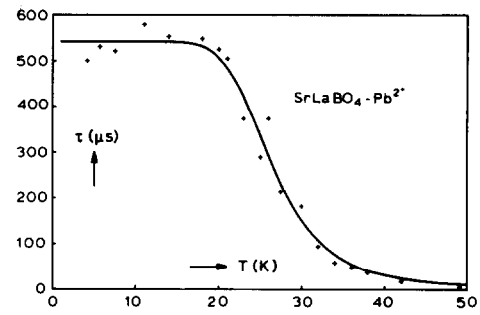

FIG. 4. Decay times of the emission of $SrLaBO_4$–Pb^{2+} as a function of temperature.

In view of the large Stokes shift of the Pb^{2+} emission in $SrLaBO_4$, energy transfer between Pb^{2+} ions mutually is highly improbable (*13, 15*). This is because the resonance condition is not fulfilled. To investigate this further we increased the Pb^{2+} concentration in $Sr_{1-x}Pb_xLaBO_4$ considerably. According to X-ray data replacement of Sr^{2+} by Pb^{2+} is possible up to $x = 0.5$. Samples with $0 < x \leq 0.5$ are all efficient luminescent materials at room temperature, i.e., no concentration quenching was observed. This agrees with the expectation that energy transfer does not take place. From Table II it can be seen that the emission maximum does not depend on the values of x, whereas the excitation maximum shifts slightly to lower energies for increasing value of x, a rather general phenomenon.

At 4.2 K we observed for $x = 0.5$ also a weak emission at 530 nm with excitation maximum at 370 nm. We assume that this is the first indication for second-phase formation, i.e., the emission is ascribed to Pb^{2+} ions in a second phase. It was not investigated further.

3.6. Sn^{2+} luminescence. Also for

$SrLaBO_4$–Sn^{2+} the decay times were measured. All decay curves are exponential. Results are shown in Fig. 5. The drawn curve was fitted as described above with the following parameters: $\Delta E_{23} = (178 \pm 11)$ cm^{-1}, $\tau_0 = (301 \pm 5)$ μsec and $\tau_1 = (2 \pm 1)$ μsec. The value of τ_1 is one order of magnitude larger than the one for $SrLaBO_4$–Pb^{2+}. This agrees with the stronger spin–orbit coupling in the case of the Pb^{2+} ion. It is this coupling which lifts the spin-selection-rule on the $^3P_1 \rightarrow {}^1S_0$ transition. The value of ΔE_{23} is unexpectedly large for Sn^{2+}. For KI–Sn^{2+} $\Delta E_{23} = 34$ cm^{-1} has been reported (*17*). In view of the lack of structural data, we have to abandon further discussion.

3.7. Energy transfer from Pb^{2+} to Eu^{3+} and Tb^{3+}. Samples (Sr,Pb)[La,Eu(Tb)]BO_4 were investigated for energy transfer from Pb^{2+} to Eu^{3+} or Tb^{3+}. This transfer was found to have a low probability. Even for 5% Eu^{3+} or Tb^{3+}, excitation into the Pb^{2+} ion results in an emission which consists for about 50% of Pb^{2+} emission. Since the Pb^{2+} excitation band overlaps those for Eu^{3+} and Tb^{3+}, the greater part of the rare-earth emission observed is probably due to direct excitation. Because energy transfer between Pb^{2+} ions does not take place, we have only to evaluate the $Pb^{2+} \rightarrow Eu^{3+}$ (Tb^{3+}) transfer process.

For electric dipole–dipole interaction the critical distance for this transfer can be found from (Refs. (*18, 19*)

$$R_c^6 = 0.63 \times 10^{28} \frac{Q_A}{E^4} \int f_s(E) f_A(E) dE.$$

Here Q_A is the absorption cross section of the rare-earth ion and E the energy where maximum overlap between emission and absorption occurs. The integral presents the spectral overlap between emission and absorption. For Q_A we took as an upper maximum 25×10^{-22} cm^2 eV (*19*). The spectral overlap is less than 0.02 eV^{-1}. With these data we find as an upper limit $R_c = 3$ Å. Although the crystal structure is not known, the sizes of the Sr^{2+} and La^{3+} ions in high coordination prevent the Pb^{2+} and Eu^{3+}(Tb^{3+}) to be so close together. The inefficiency of the transfer is, therefore, not unexpected.

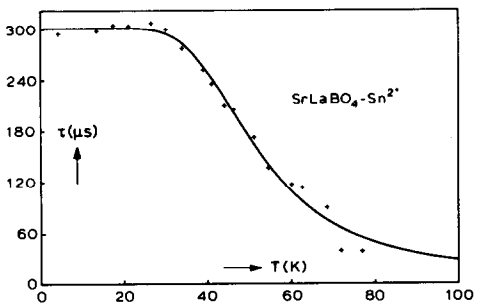

FIG. 5. Decay times of the emission of $SrLaBO_4$–Sn^{2+} as a function of temperature.

3.8. Impurity emission. In practically all our samples we observed a weak, deep-red emission. It was most intense in a manganese-doped $SrLaBO_4$ sample. Since the spectra correspond to Mn^{4+}, we ascribe the emission to Mn^{4+}, which must be present in one of our starting materials (e.g., $SrCO_3$). It cannot be excluded that the activator is present in a second phase which is present at low concentration, since the excitation is only possible where the other activators are not excitable. The quantum efficiency of this luminescence is high and no thermal quenching is observed. The emission consists at 4.2 K of a number of sharp lines, situated at 700, 709, 718, and 726 nm. At 300 K these broaden considerably. This may be the $^2E \rightarrow {}^4A_2$ transition. The excitation consists of a sharp line at 614 nm ($^4A_2 \rightarrow {}^2T_2$), and bands at 470 nm ($^4A_2 \rightarrow {}^4T_2$), ~380 nm ($^4A_2 \rightarrow {}^4T_1$), and 345 nm (charge transfer). We refrain from further discussion in view of lack of structural data.

Acknowledgments

The authors are indebted to G. J. Dirksen for useful

advice during the preparation and to P. A. M. Berdowski for decay time measurements.

References

1. W. H. M. M. VAN DE SPIJKER AND W. L. KONIJNENDIJK, *Inorg. Nucl. Chem. Lett.* **14,** 389 (1978).
2. C. W. M. TIMMERMANS AND G. BLASSE, *J. Solid State Chem.* **52,** 222 (1984).
3. H. RONDE AND G. BLASSE, *J. Inorg. Nucl. Chem.* **40,** 136, 215 (1978).
4. H. SIEBERT, "Anwendungen der Schwingungsspektroskopie in der Anorganischen Chemie," p. 53, Springer-Verlag, Berlin (1966).
5. J. P. LAPERCHES AND P. TARTE, *Spectrochim. Acta* **22,** 1201 (1966).
6. G. BLASSE, *J. Inorg. Nucl. Chem.* **31,** 1519 (1969).
7. L. A. HARRIS AND H. L. YAKEL, *Acta Crystallogr.* **22,** 354 (1967).
8. H. E. HOEFDRAAD, *J. Solid State Chem.* **15,** 175 (1975).
9. G. BLASSE AND S. KEMMLER-SACK, *Ber. Bunsenges.* **87,** 698 (1983).
10. W. C. NIEUWPOORT AND G. BLASSE, *Solid State Commun.* **4,** 227 (1966).
11. S. N. RUDDLESDEN AND P. POPPER, *Acta Crystallogr.* **10,** 538 (1957).
12. G. BLASSE, *J. Inorg. Nucl. Chem.* **27,** 993 (1965).
13. G. BLASSE, *in* "Handbook on the Physics and Chemistry of Rare Earths" (K. A. Gschneider and L. Eyring, Eds.), Chap. 34, North-Holland, Amsterdam (1979).
14. G. BLASSE AND A. BRIL, *J. Chem. Phys.* **47,** 5139 (1967).
15. G. BLASSE, *in* "Luminescence of Inorganic Solids" (B. DiBartolo, Ed.), p. 457 sq. Plenum, New York (1978).
16. G. BLASSE, *Chem. Phys. Lett.* **104,** 160 (1984).
17. LE SI DANG, P. W. M. JACOBS, K. SCHMITT, V. S. SIVASANKAR, AND D. J. SIMKIN, *Chem. Phys.* **66,** 51 (1982).
18. D. L. DEXTER, *J. Chem. Phys.* **21,** 836 (1953).
19. G. BLASSE, *Philips Res. Rep.* **24,** 131 (1969).